Scilight

Thermal Science and Applications
https://www.sciltp.com/journals/tsa

Article

Analysis and Control of a Boiling Water Reactor Model

Lakshmi N. Sridhar

Chemical Engineering Department, University of Puerto Rico, Mayaguez, PR 00681, USA; lakshmin.sridhar@upr.edu

How To Cite: Sridhar, L.N. Analysis and Control of a Boiling Water Reactor Model. *Thermal Science and Applications* **2025**, *1*(1), 21–32.

Received: 25 September 2026
Revised: 19 December 2026
Accepted: 22 December 2026
Published: 30 December 2026

Abstract: The Boiling Water Reactor (BWR) problem is a highly nonlinear physical system, and one must understand the dynamics in order to effectively control it. In this research, bifurcation analysis and multiobjective nonlinear model predictive control are performed on a boiling water reactor model. Bifurcation analysis is a powerful mathematical tool used to deal with the nonlinear dynamics of any process. Several factors must be considered, and multiple objectives must be met simultaneously. The MATLAB program MATCONT was used to perform the bifurcation analysis. The MNLMPC calculations were performed using the optimization language PYOMO in conjunction with the state-of-the-art global optimization solvers IPOPT and BARON. The bifurcation analysis revealed the existence of Hopf bifurcations. The Hopf bifurcations, which cause unwanted limit cycles, are eliminated with the use of the tanh functions. The MNLMPC calculations converge to the best possible solution, which is referred to as the Utopia point.

Keywords: bifurcation analysis; dynamic optimization; nuclear; neutron

1. Introduction

A Boiling Water Reactor, abbreviated as BWR, is a type of Light Water Nuclear Reactor that uses ordinary water as both a coolant and moderator, which converts nuclear energy released from atoms into electricity in a steam-powered turbine. BWRs are similar in design to Graphite Gas Cooled Reactors but without a separate cooling plant. BWRs are also similar in design to Pressurized Water Reactors. In BWRs, freshwater is pumped from the bottom of the reactor vessel and rises through a core where it absorbs heat from nuclear fission that takes place in nuclear fuel assemblies consisting of enriched uranium. As a result, heated water turns into a steam-water mixture near the top of the vessel. The steam, in a BWR, passes through a series of moisture separators and dryers located above the reactor core to ensure that dry steam reaches the turbine. Because steam in a BWR is produced in the reactor vessel, there would be slightly radioactive steam in a turbine-generator set, which would require additional shielding and plant operation strategies. A characteristic of a BWR, in relation to other reactor designs, is that it has a relatively easy design. Unlike a Pressurized Water Reactor, BWRs are also devoid of massive pressurizers and steam generators because steam booms in BWRs when operating under normal reactor pressure. This design reduces the total number of major components, reduces reactor pressure compared to that in a Pressurized Water Reactor, and also increases in-built reactor safety in certain conditions. In a BWR, control rods are moved from below a reactor core. This allows for control over nuclear fission rates, hence reactor powers. Moreover, in a BWR, a mechanism in which “more steam voids make a reactor less reactive” acts as a natural control mechanism in a reactor, known as a void coefficient of reactivity, which provides for a higher rate of boiling that decreases reactivity.

BWR designs have gone through several generations, with the latest variants boasting advanced safety systems, better fuel economy, and passive cooling. They are in service all over the world and have a reputation for being reliable, efficient sources of baseload power. In nuclear technology, they are unique due to their method of direct-cycle steam generation, which is at the heart of most large-scale power plants. BWRs are quite popular in nuclear energy production owing to their efficiency, reliability, and simplicity of design. Unlike other types of Pressurized Water Reactors, BWRs facilitate direct boiling of water in a reactor vessel, which then expands as

steam to activate the turbine. Needless to say, this design of a direct cycle reduces the complexity of components in a system. BWRs also pose a decreased risk of accidents.

One of the major advantages of BWRs is their natural stability in operation. Since steam generation takes place in the core, any variation in reactor power output gets naturally compensated by the formation of steam bubbles, which in turn slow down the rate of reaction. This property, known as a negative void coefficient, suppresses any surge in reactor power, which has improved their enhanced safety features as well as their potential for rapid load variation.

BWRs also provide a good fuel economy. This is due to their design, which allows for a high efficiency rate, enabling a substantial amount of nuclear fission energy to be converted into electricity. Furthermore, present-day fuel assemblies for BWRs use advanced fuel geometries that enhance fuel cycles and fuel management, hence promoting a sustainable nuclear program.

Boiling Water Reactor technology has almost sixty years of experience, which ensures a proven track record of performance and development of supply chains. On a whole, Boiling Water Reactors are a very useful and reliable technology for generating large-scale, low-carbon electricity that would cater to the increasing needs of the world.

Boiling water reactors, although valuable contributors to nuclear energy production, have a number of associated hazards that need careful management for safe operation. First among these concerns is the direct cycle design where water actually boils inside the reactor vessel. The steam produced in the core, which then goes directly to the turbine, can take radioactive contaminants with it. While filtration and shielding systems reduce this risk, it still means parts of the turbine hall have to be subject to more stringent radiation controls than those of other reactor types.

Another risk involves accidents of the loss-of-coolant type. Because water in a boiling-water reactor serves both as coolant and moderator, any major loss of water inventory can reduce heat removal from the fuel. While contemporary safety systems would work to damp such incidents, failure of cooling can lead to overheating of fuel rods and, in extreme cases, partial meltdowns.

BWRs also face risks associated with pressure vessel aging and material degradation. Over decades of operation, components are exposed to intense neutron radiation at high temperatures, with corrosion. These factors can weaken structural materials and increase the chance of leaks or equipment malfunction.

The BWR operates on the principle of maintaining balance among water levels, steam production, and reactivity; and any one factor would lead to unsafe conditions. The development of automation does make the operation more reliable. However, this automation must be programmed to avoid Hopf bifurcation causing limit cycles. These Hopf bifurcations are caused because of the nonlinearity of the BWR process. The source of nonlinearity in a boiling water reactor (BWR) plant process can be traced back to the complex interactions between neutron kinetics, thermohydraulics, and two-phase flow phenomena. With a rise in reactor power, additional steam bubbles are produced in the core, which, in turn, decreases the moderator density of a BWR with a nonlinear effect on neutron moderation. This void reactivity feedback mechanism is known to be neither proportional nor direct, resulting in quite complex dynamic effects. There are also couplings between fuel, steam, and coolant convective heat transfers, which are a function of certain properties that are temperature-dependent, giving rise to additional nonlinearities. The main purpose of this paper is to demonstrate effective strategies to avoid the Hopf bifurcations and limit cycles from occurring. The incorporation of the tanh function in the manipulated variables will definitely help in avoiding the Hopf bifurcations and limit cycles and that is the central message of this paper.

2. Literature Review

March-Leuba et al. [1,2] investigated the nonlinear dynamics and instability of boiling water reactors. Munoz-Cobo et al. [3] discussed the use of Hopf bifurcation theory and calculus of variations to the study of the formation of limit cycles in boiling water reactors. Wang et al. [4] provided an analysis on the mathematical structure of the nonlinear BWR model. Tsuji et al. [5] discussed the stability analysis of BWRs using bifurcation theory. Rizwan-uddin et al. [6] demonstrated the existence of limit points and subcritical and supercritical bifurcation points in a simple BWR model. Lange et al. [7] developed an advanced model for BWR reducing the order and conducting stability analysis. Wahi et al. [8] performed Lyapunov stability studies of nuclear reactors reducing the order of the equations. Bindra et al. [9], and Pandey et al. [10] studied the effects of modelling assumptions on the stability domains of BWRs and provided a detailed bifurcation analysis with a modified model for the advanced heavy water reactor system. Pandey et al. [11] performed nonlinear analysis of boiling water reactors in a substantial domain of parametric spaces.

All the work so far involving BWR focused on bifurcation analysis or optimal control performed disjointly. In this work, bifurcation studies and multiobjective nonlinear model predictive control are performed on a boiling water nuclear reactor model [11]. The paper is presented as in this manner. The model equations that represent this model are first presented. This is followed by a discussion of the computational procedures regarding bifurcation analysis and multiobjective nonlinear model predictive control (MNLMPC). The results, discussion and conclusions are then presented.

The novelty of this work lies in the integration of bifurcation analysis and optimal control of the BWR model. Normally, both bifurcation analysis and optimal control are performed individually. This work represents the first attempt to combine these two computational tasks and apply them to boiling water reactors.

3. Model Equations

The variables involved are ($nv(t)$; $cv(t)$; $tv(t)$; $\rho a(t)$; $\rho t(t)$) and they represent the excess neutron population, excess population of delayed neutron precursors, excess fuel temperature, excess void reactivity feedback, and the derivative of the excess void reactivity feedback with time, respectively. All the parameters have been obtained from the nuclear properties and the reactor's geometry. The model equations are

$$\begin{aligned}
\frac{d(nv)}{dt} &= 2\frac{\rho a}{\lambda_c} + 2d\left(\frac{tv}{\lambda_c}\right) - \frac{\beta}{\lambda_c} + \lambda_s(cv) \\
\frac{d(cv)}{dt} &= \frac{\beta}{\lambda_c} nv - \lambda_c(cv) \\
\frac{d(tv)}{dt} &= a_1(nv) - a_2(tv) \\
\frac{d(\rho a)}{dt} &= \rho t \\
\frac{d(\rho t)}{dt} &= k(tv) - a_3(\rho t) - a_4(\rho a)
\end{aligned} \tag{1}$$

The base parameters are

$$a_1 = 25.04;\ a_2 = 0.23;\ a_3 = 2.25;\ a_4 = 6.82;\ k = -3.7 \times 10^{-3};$$
$$d = -2.52 \times 10^{-5};\ \beta = 0.0056; \lambda_c = 4.0 \times 10^{-5}; \lambda_s = 0.08.$$

Details can be found in Pandey and Singh ([10,11]).

4. Bifurcation Analysis

Bifurcation calculations are performed using the MATLAB software MATCONT. Bifurcation analysis explains the main causes for multiple steady-states and limit cycles. Branch points and limit points cause multiple steady-state solutions while limit cycles and oscillatory behavior are caused by Hopf bifurcation points. The MATLAB program that effectively locates limit points, branch points, and Hopf bifurcation points is MATCONT. This program was developed and improved by several researchers ([12,13]). This program is very effective in identifying Limit points (LP), branch points (BP), and Hopf bifurcation points (H) for a system of ordinary differential equations

$$\frac{dx}{dt} = f(x, \alpha) \tag{2}$$

$x \in R^n$ where the bifurcation parameter is α. The gradient vector is orthogonal to the tangent and hence the tangent plane at any point $w = [w_1, w_2, w_3, w_4, \ldots, w_{n+1}]$ must satisfy

$$Aw = 0 \tag{3}$$

The matrix A is defined by

$$A = [\partial f / \partial x \quad | \partial f / \partial \alpha] \tag{4}$$

The sub-matrix $\partial f/\partial x$ is the Jacobian matrix. For both limit and branch points, the Jacobian matrix $J = (\partial f/\partial x)$ must have a determinant of 0.

At a limit point, there must exist only one tangent at the point of singularity. At this singular point, there is a one and only one non-zero vector, y, where $Jy = 0$. This vector is of dimension n. Since there is only one tangent, the vector $y = (y_1, y_2, y_3, y_4, \ldots, y_n)$ must have the same direction with $\hat{w} = (w_1, w_2, w_3, w_4, \ldots, w_n)$. Since

$$J\hat{w} = Aw = 0 \tag{5}$$

the $n + 1^{th}$ component of the tangent vector $w_{n+1} = 0$. This is the necessary condition for the existence of a a limit point (LP).

For a branch point, two tangents must exist at the point of singularity. Let the two tangents be *z* and *w*. This implies that

$$\begin{aligned} Az &= 0 \\ Aw &= 0 \end{aligned} \tag{6}$$

Imagine a vector v that is orthogonal to one of the tangent w. v can be expressed as a linear combination of *z* and *w* ($v = \gamma z + \delta w$). Since $Az = Aw = 0$; $Av = 0$ and since *w* and *v* are orthogonal, $w^T v = 0$. Hence $Bv = \begin{bmatrix} A \\ w^T \end{bmatrix} v = 0$ which implies that B is singular. This implies that the necessary condition for the existence of a branch point is that the matrix $B = \begin{bmatrix} A \\ w^T \end{bmatrix}$ must be singular and have a determinant of 0.

At a Hopf bifurcation point,

$$\det(2f_x(x, \alpha) @ I_n) = 0 \tag{7}$$

@ indicates the bialternate product while I_n is the n-square identity matrix. Hopf bifurcations cause limit cycles and should be eliminated because limit cycles make optimization and control tasks very difficult. More details can be found in Kuznetsov [14–16] respectively.

Hopf bifurcations cause limit cycles. Limit cycles cause equipment damage and make control tasks etc. difficult. Additionally, they result in less beneficial products. The tanh activation function (where a control value *u* is replaced by $(u \tanh u/\varepsilon)$) is used to eliminate spikes in the optimal control profiles. Several workers demonstrated this. Refs. [17–21] explained with several examples how the same activation factor that involves the the tanh function also successfully eliminates the limit-cycle causing Hopf bifurcation points. This was because the tanh function increases the oscillation time period in the limit cycle.

5. Multiobjective Nonlinear Model Predictive Control (MNLMPC)

Flores Tlacuahuaz et al. [22] originally developed a rigorous multiobjective nonlinear model predictive control (MNLMPC) strategy. This procedure is used for performing the MNLMPC calculations. used. In a problem for which the variables $\sum_{t_{i=0}}^{t_i=t_f} q_j(t_i); j = 1,2, \ldots, n$ have to be optimized simultaneously, and the dynamic model is given by

$$\frac{dx}{dt} = F(x, u) \tag{8}$$

t_f being the final time value, and n the total number of objective variables and *u* the control parameter. The single objective optimal control problem is solved independently for each of the variables $\sum_{t_{i=0}}^{t_i=t_f} q_j(t_i)$ and produces the values q_j^*. Then, the multiobjective optimal control (MOOC) problem that will be solved is

$$\begin{aligned} &\min\left(\sum_{j=1}^{n}\left(\sum_{t_{i=0}}^{t_f} q_j(t_i) - q_j^*\right)\right)^2 \\ &\text{subject to } \frac{dx}{dt} = F(x, u); \end{aligned} \tag{9}$$

This will provide the values of *u* at various times. The first obtained control value of *u* is implemented and the rest are discarded. This procedure is repeated until the implemented and the first obtained control values are the same or if the Utopia point where $(\sum_{t_{i=0}}^{t_f} q_j(t_i) = q_j^*;\ j = 1,2, \ldots, n)$ is obtained.

The Utopia point is one where all the objectives are met, even if they are conflicting.

Pyomo.dae [23] is used for these calculations. Here, the differential equations are converted to a Nonlinear Program (NLP) using the orthogonal collocation method.

The NLP is solved using IPOPT [24] and confirmed as a global solution with BARON [25].

6. Integration of Bifurcation Analysis and Optimal Control

The main contribution of this paper lies in the integration of bifurcation analysis and optimal control. From a mathematical standpoint, this integration is relatively new and has never been done for boiling water reactor systems (BWR). Why is such an integration important? The BWR is a very nonlinear process and to be able to operate it effectively, avoiding wastage of resources, one must be able to control it effectively. Otherwise, the process may blow up, causing damage to life and property and result is colossal wastage of money and equipment, not to mention any of the resulting environmental disasters.

The intuitive reason for linking bifurcation analysis and optimal control is as follows. Bifurcation analysis involves singularities, which are classified as branch points, limit points and Hopf bifurcation points. Optimal control involves the location of maxima and minima, which are also singularities. It therefore stands to reason that these two very important fields in applied mathematics must be related.

The singularities occur because of the nonlinear nature of the boiling water reaction process. One of the main symptoms of this nonlinearity is the existence of spikes in the control profile. There are a few ways of eliminating the spikes, which are also referred to as noise. The use of filters like the Savitzky-Golay filter is a common method. However, the use of the filters requires that we first have all the data before the filter can be applied. Filters cannot prevent spikes (noise) as they occur. The tanh activation factor successfully stifles the spikes as they occur. Spikes are just nonsmoothed oscillations. If the tanh function eliminates spikes it stands to reason that they should be effective in eliminating oscillations also. This work clearly demonstrates that the activation factor involving the tanh function effectively eliminates the oscillatory behavior and the limit cycles which are caused by the Hopf bifurcations. The product of the tanh function and the manipulated variable can be implemented in control tasks and effectively prevent limit cycles which are wasteful and hazardous.

All nuclear reactors exhibit limit cycles which are unwanted and dangerous. It is essential to avoid them. This can only be achieved by the elimination of the Hopf bifurcations that cause them. The results clearly indicate that the tanh function is very effective in eliminating the Hopf bifurcations. The tanh function can be used in control tasks for other types of nuclear reactors, such as heavy water nuclear reactors as well.

7. Results and Discussion

Bifurcation analysis is performed with several bifurcation parameters. In each of the cases, the use of an activation factor involving the tanh function removes the unwanted limit cycle causing Hopf bifurcations validating the hypothesis of Sridhar (2024) [21].

(1) When a_1 is the bifurcation parameter, 2 Hopf bifurcation points are found at $(nv,\ cv,\ tv,\ \rho a,\ \rho t,\ a_1)$ values of (0.0005, 1750.294863, 0.000831, 0, 0, 0.382198) and (0.0005, 1750.318326, 0.000897, 0, 0, 0.412605) (curve AB in Figure 1a). When a_1 is changed to $a_1\tanh(a_1)/10$ the Hopf bifurcations disappear (curve CD in Figure 1a). The limit cycles for these two Hopf bifurcation points are shown in Figure 1b,c.

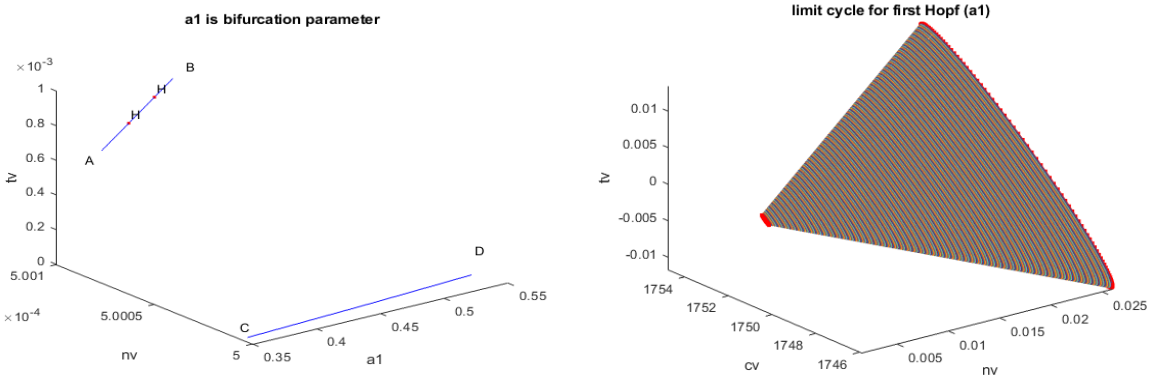

(**a**) (**b**)

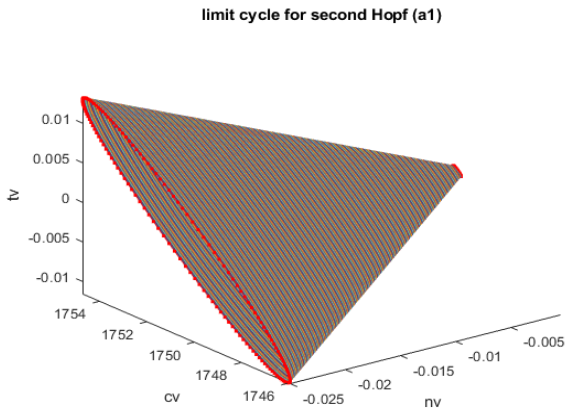

(**c**)

Figure 1. (**a**) bifurcation diagram with a_1 as bifurcation parameter; (**b**) limit cycle for the first Hopf bifurcation with a_1 as bifurcation parameter; (**c**) limit cycle for the second Hopf bifurcation with a_1 as bifurcation parameter.

(2) When a_2 is the bifurcation parameter, a Hopf bifurcation point are found at $(nv,\ cv,\ tv,\ \rho a,\ \rho t,\ a_2)$ values of (0.0005, 1750.039114, 0.000110, 0, 0, 113.579623) (curve AB in Figure 2a). When a_2 is changed to $a_2\tanh(a_2)/10$ the Hopf bifurcation disappears (curve CD in Figure 2a). The limit cycle for this Hopf bifurcation points are shown in Figure 2b

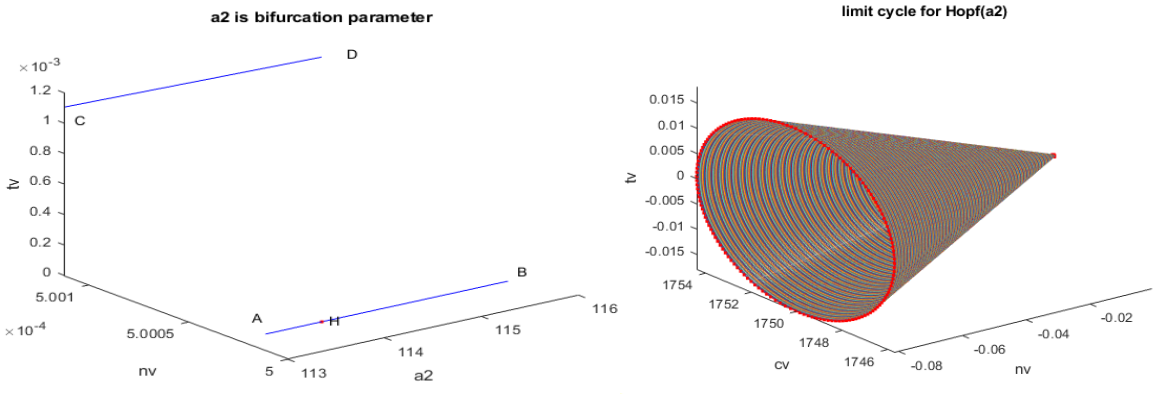

(**a**) (**b**)

Figure 2. (**a**) bifurcation diagram with a_2 as bifurcation parameter; (**b**) limit cycle for the first Hopf bifurcation with a_2 as bifurcation parameter.

(3) When a_3 is the bifurcation parameter, a Hopf bifurcation point are found at $(nv,\ cv,\ tv,\ \rho a,\ \rho t,\ a_3)$ values of (0.000506, 1769.530449, 0.055042, 0.000030, 0, −0.221188) (Figure 3a). When a_3 is changed to $a_3\tanh(a_3)/10$ the Hopf bifurcation disappears (Figure 3b). The limit cycle for this Hopf bifurcation points are shown in Figure 3c (2-dimensional) and 3d (3-dimensional).

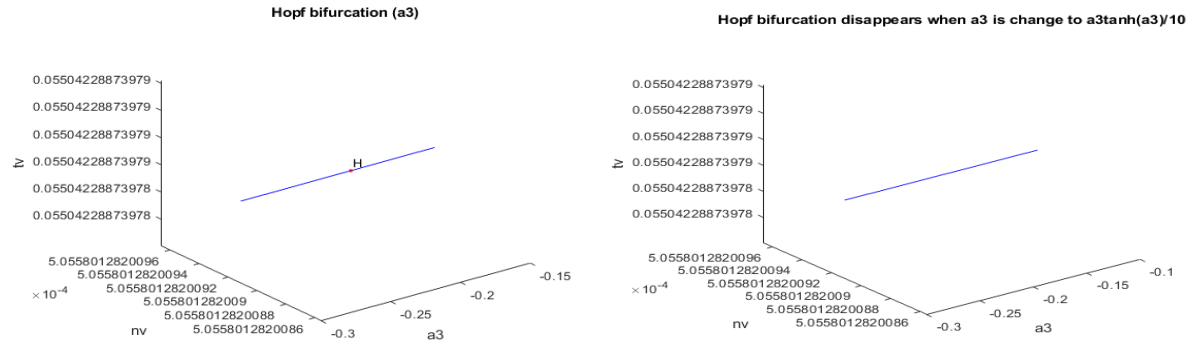

(**a**) (**b**)

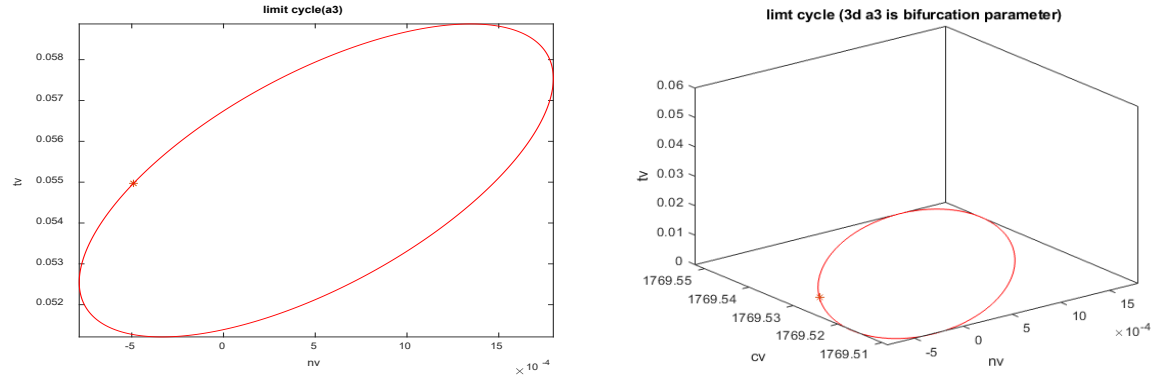

(**c**) (**d**)

Figure 3. (**a**) Hopf bifurcation with a$_3$ as bifurcation parameter; (**b**) Hopf bifurcation disappears when a_3 is changed to $a_3\tanh(a_3)/10$; (**c**) limit cycle for the first Hopf bifurcation with a_3 as bifurcation parameter 2-dimensional; (**d**) limit cycle for the first Hopf bifurcation with a_3 as bifurcation parameter 3-dimensional.

(4) When a_4 is the bifurcation parameter, a Hopf bifurcation point are found at $(nv,\ cv,\ tv,\ \rho a,\ \rho t, a_4)$ values of (0.0005, 1751.395615, 0.054478, −0.000001, 0, 234.346715) (curve AB in Figure 4a). When a_4 is changed to $a_4\tanh(a_4)/10$ the Hopf bifurcation disappears (curve CD in Figure 4a). The limit cycle for this Hopf bifurcation point is shown in Figure 4b.

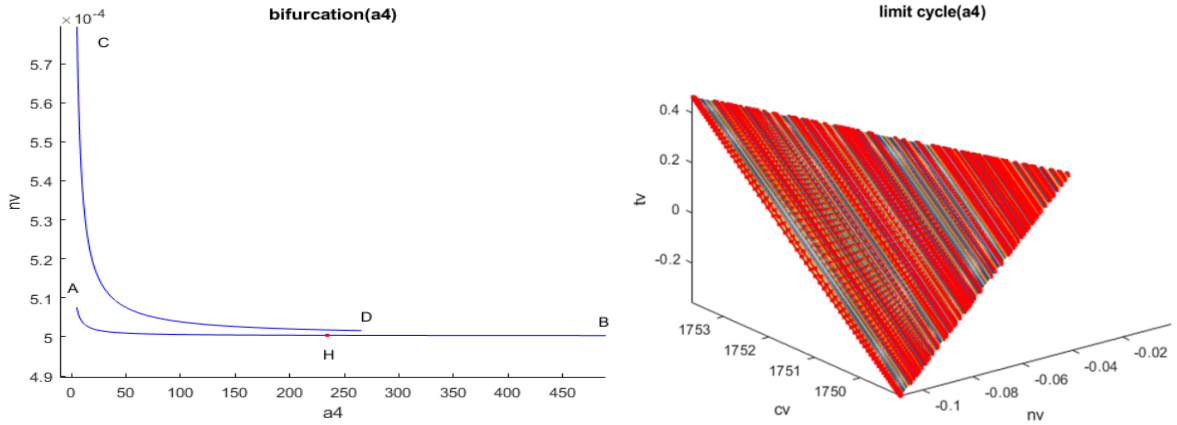

(**a**) (**b**)

Figure 4. (**a**) bifurcation diagram with a_4 as bifurcation parameter; (**b**) limit cycle with a_4 as bifurcation parameter.

(5) When k is the bifurcation parameter, a Hopf bifurcation point are found at $(nv,\ cv,\ tv,\ \rho a,\ \rho t, k)$ values of (0.0005, 1751.007448, 0.054466, 0, 0, −0.000030) (curve AB in Figure 5a). When k is changed to $k\tanh(k)/10$ the Hopf bifurcation disappears (curve CD in Figure 5a). The limit cycle for this Hopf bifurcation point is shown in Figure 5b.

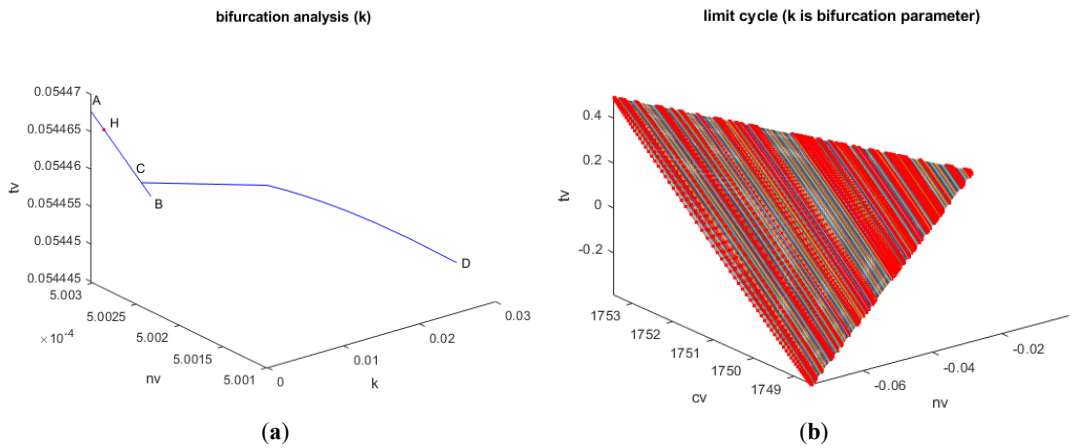

(**a**) (**b**)

Figure 5. (**a**) bifurcation diagram with k as the bifurcation parameter; (**b**) limit cycle with k as the bifurcation parameter.

(6) When d is the bifurcation parameter, a Hopf bifurcation point are found at $(nv,\ cv,\ tv,\ \rho a,\ \rho t,\ d)$ values of (0.0005, 1750.296964, 0.054444, −0.000030, 0, 0.000534) (curve AB in Figure 6a). When d is changed to $d\tanh(d)/0.001$ the Hopf bifurcation disappears (curve CD in Figure 5a). The limit cycle for this Hopf bifurcation point is shown in Figure 6b.

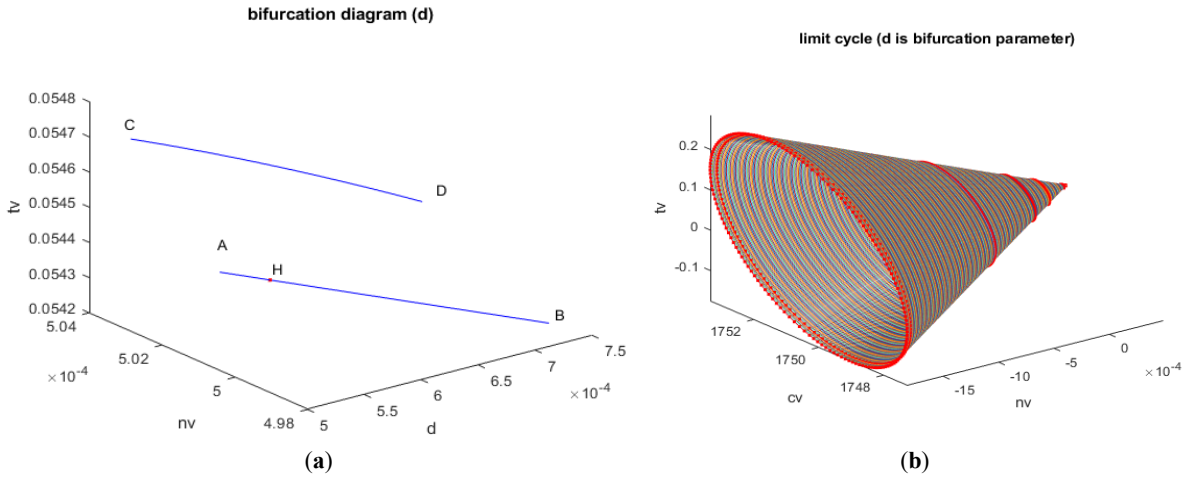

(**a**) (**b**)

Figure 6. (**a**) bifurcation diagram with d as the bifurcation parameter; (**b**) limit cycle with d as the bifurcation parameter.

(7) When λs is the bifurcation parameter, a Hopf bifurcation point are found at $(nv,\ cv,\ tv,\ \rho a,\ \rho t,\ \lambda_s)$ values of (−0.000004, −12.651797, −0.000394, 0.000000, 0.000000, −11.064739) (Figure 7a).When λ_s is changed to $\lambda_s \tanh(\lambda_s)/10$ the Hopf bifurcation disappears (Figure 7b). The limit cycle for this Hopf bifurcation point is shown in Figure 7c.

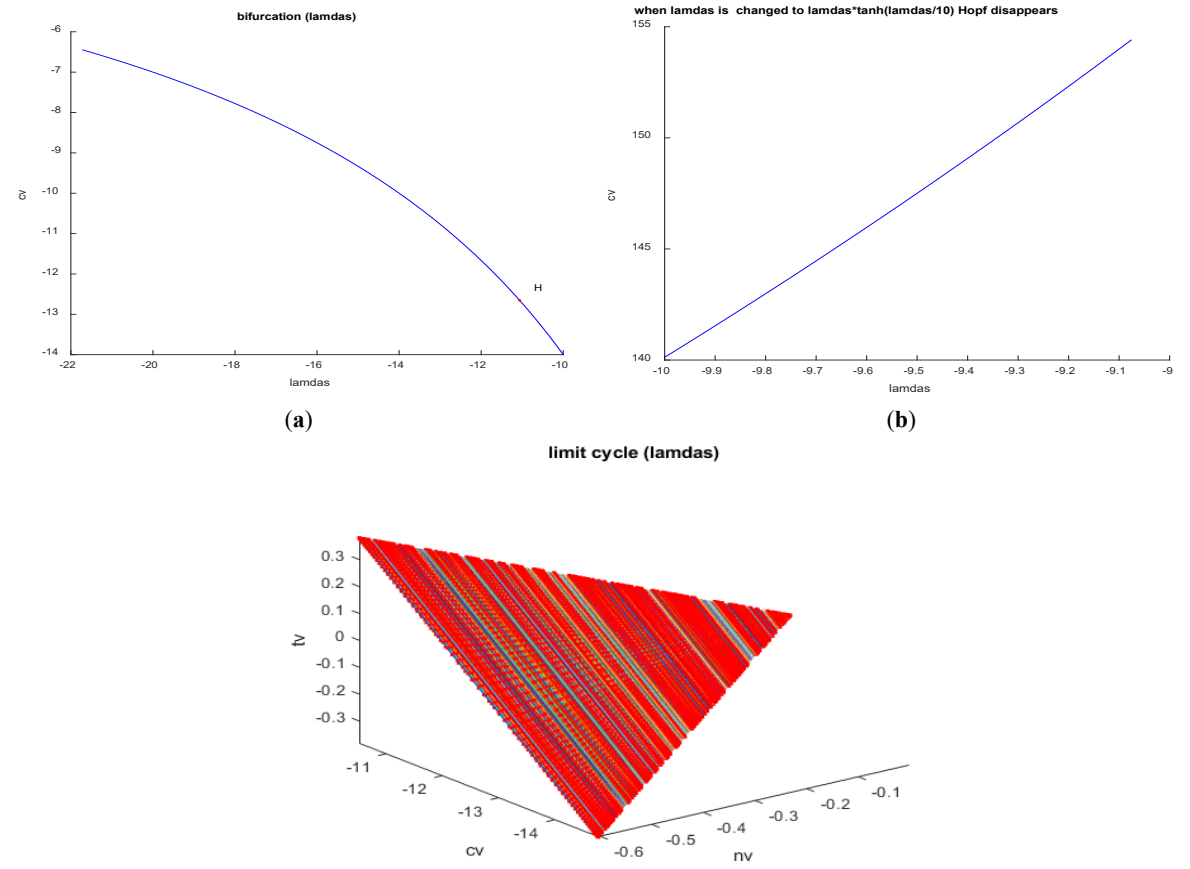

(**a**) (**b**)

(**c**)

Figure 7. (**a**) bifurcation diagram with λ_s as the bifurcation parameter; (**b**) When λ_s is changed to $\lambda_s \tanh(\lambda_s)/10$ the Hopf bifurcation disappears; (**c**) limit cycle when λ_s is the bifurcation parameter.

(8) When λ_c is the bifurcation parameter, a Hopf bifurcation point are found at $(nv,\ cv,\ tv,\ \rho a,\ \rho t,\ \lambda_c)$ valuesof (−0.049444, −0.147982, −5.382997, 0.002920, 0, 0.043256) (curve AB in Figure 8a). When λ_c is changed to $\lambda_c \tanh(\lambda_c)/10$ the Hopf bifurcation disappears (curve CD in Figure 8a). The limit cycle for this Hopf bifurcation point is shown in Figure 8b.

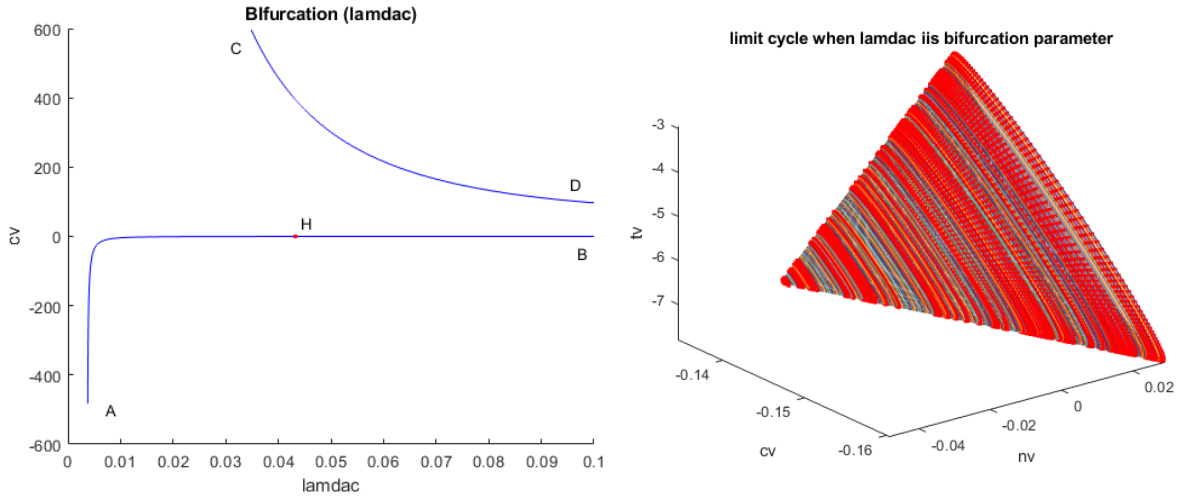

(**a**) (**b**)

Figure 8. (**a**) bifurcation diagram with λ_c as the bifurcation parameter; (**b**) limit cycle with λ_c as the bifurcation parameter.

For the MNLMPC calculations, λ_s is the control parameter, and $\sum_{t_{i=0}}^{t_i=t_f} nv(t_i)$, $\sum_{t_{i=0}}^{t_i=t_f} cv(t_i)$, $\sum_{t_{i=0}}^{t_i=t_f} tv(t_i)$ were minimized individually, and each of them led to a value of 0, 140.845, and 0. The overall optimal control problem will involve the minimization of $(\sum_{t_{i=0}}^{t_i=t_f} nv(t_i) - 0)^2 + (\sum_{t_{i=0}}^{t_i=t_f} cv(t_i) - 140.845)^2 + (\sum_{t_{i=0}}^{t_i=t_f} tv(t_i) - 0)^2$ subject to the equations governing the model. This led to a value of 0. The MNLMPC values of the control variable, λ_s is 1.9765. The MNLMPC profiles are shown in Figure 9a–f.

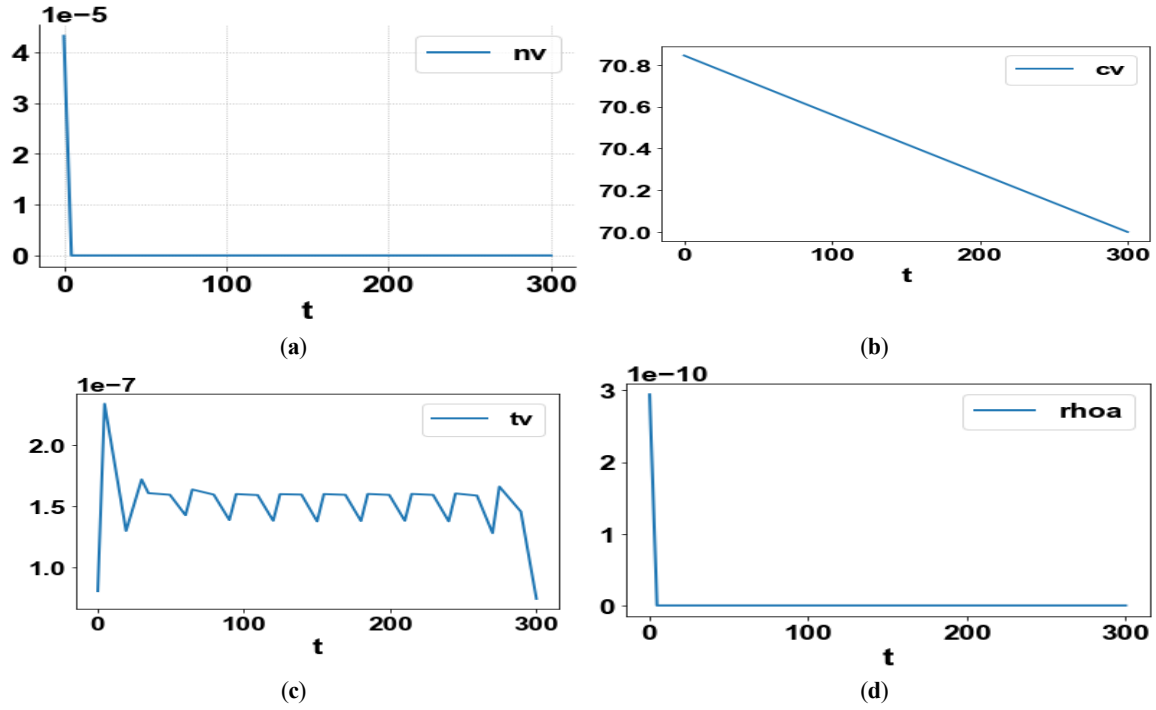

(**a**) (**b**)

(**c**) (**d**)

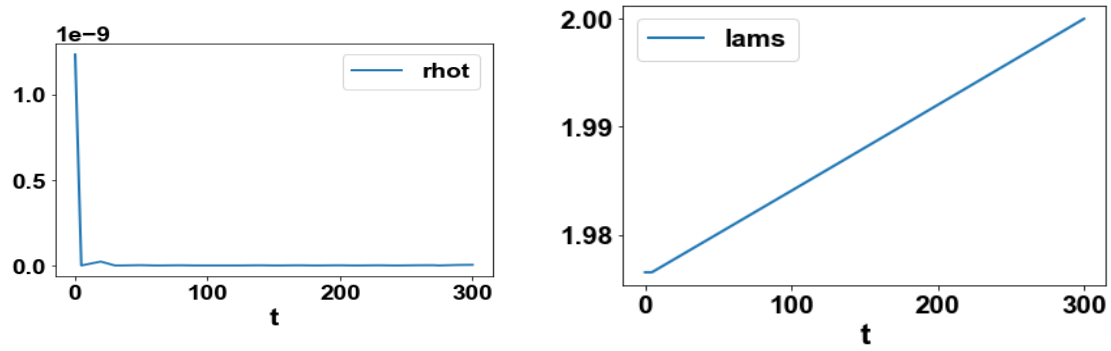

(**e**) (**f**)

Figure 9. (**a**) MNLMPC *nv* vs. *t*; (**b**) MNLMPC *cv* vs. *t*; (**c**) MNLMPC *tv* vs. *t*; (**d**) MNLMPC ρa vs. t; (**e**) MNLMPC ρe vs. t; (**f**) MNLMPC λs vs. t.

So far, all research have reported the existence of the unwanted Hopf bifurcations in BWR problems. This work is the first in open literature where strategies to eliminate them are presented. One of the primary objectives of this research is to demonstrate the effectiveness of the tanh function in eliminating Hopf bifurcations that lead to limit cycles. Limit cycles cause self-sustained oscillations in variables like neutron flux, core power, steam generation, and two-phase coolant flow. These repeat with a non-significant amplitude and period instead of decaying exponentially. The existence of limit cycles demonstrates that destabilizing feedbacks are overriding the stabilizing ones. Boiling water reactors operate with two-phase flow. This causes certain regions of the core to experience stronger void responses or weaker cooling during parts of the cycle. This can push local conditions close to or beyond thermal limits, endangering safety and causing severe equipment damage. In BWRs, where power production is directly tied to boiling behavior and strong coupling exists between neutron kinetics and two-phase flow, limit cycles create conditions that threaten fuel integrity, operational stability, and overall plant safety. One of the most serious consequences of limit cycles in BWRs is the increased risk of localized fuel damage. Oscillatory power leads to oscillatory heat flux and temperature at the fuel-cladding interface. This accelerates cladding corrosion, pellet–cladding mechanical interaction, and thermal fatigue. The tanh function is normally used to eliminate spikes in control profiles. Spikes are very similar to periodic oscillations. However, spikes exist in the manipulated variables. The periodic oscillations exist in the output variables and are damaging. This result has many practical implications. If the control engineer incorporates the tanh function in the manipulated variable, the Hopf bifurcations and the limit cycles won't occur, resulting in safety and preventing equipment damage. This, along with the multi-objective nonlinear model predictive control, will provide strategies to achieve the most beneficial result, prioritizing safety, reducing resource wastage, and minimizing expenses. The rising cost of energy requires that all wastage be reduced to a minimum.

8. Conclusions

Bifurcation analysis and multiobjective nonlinear control (MNLMPC) studies on a boiling water nuclear reactor model. The bifurcation analysis revealed the existence of a Hopf bifurcation point The Hopf bifurcation point, which causes an unwanted limit cycle, is eliminated using an activation factor involving the tanh function. The MNLMPC calculations resulted in the Utopia (the best possible) solution A combination of bifurcation analysis and Multiobjective Nonlinear Model Predictive Control (MNLMPC) for a boiling water nuclear reactor model is the main contribution of this paper.

Funding

This research received no external funding.

Institutional Review Board Statement

Not applicable.

Informed Consent Statement

Not applicable.

Data Availability Statement

All data used is presented in the paper.

Acknowledgments

Sridhar thanks Carlos Ramirez and Suleiman for encouraging him to write single-author papers.

Conflicts of Interest

The author declares no conflict of interest.

Use of AI and AI-Assisted Technologies

No AI tools were utilized for this paper.

References

1. March-Leuba, J.; Cacuci, D.G.; Perez, R.B. Nonlinear dynamics and stability of boiling water reactors: Part 1—Qualitative analysis. *Nucl. Sci. Eng.* **1986**, *93*, 111–123.
2. March-Leuba, J.; Cacuci, D.G.; Perez, R.B. Nonlinear dynamics and stability of boiling water reactors: Part 2—Qualitative analysis. *Nucl. Sci. Eng.* **1986**, *93*, 124–136.
3. Munoz-Cobo, J.L.; Verdu, G. Application of Hopf bifurcation theory and variational methods to the study of limit cycles in boiling water reactors. *Ann. Nucl. En*ergy **1991**, *18*, 269–302.
4. Wang, H.; Kondo, S. Analysis on the mathematical structure of nonlinear BWR model. *Nucl. Eng. Des.* **1992**, *137*, 267–274.
5. Tsuji, M.; Nishio, K.; Narita, M. Stability analysis of BWRs using bifurcation theory. *J. Nucl. Sci. Technol.* **1993**, *30*, 1107–1119.
6. Rizwan-Uddin. Turning points and sub- and supercritical bifurcations in a simple BWR model. *Nucl. Eng. Des.* **2006**, *236*, 267–283.
7. Lange, C.; Hennig, D.; Hurtado, A. An advanced reduced order model for BWR stability analysis. *Prog. Nucl. Energy* **2011**, *53*, 139–160.
8. Wahi, P.; Kumawat, V. Nonlinear stability analysis of reduced order model of nuclear reactors- A parametric study relevant to the AHWR. *Nucl. Eng. Des.* **2011**, *241*, 134–143.
9. Bindra, H. Effects of modelling assumptions on the stability domains of BWRs. *Ann. Nucl. Energy* **2014**, *67*, 13–20.
10. Pandey, V.; Singh, S. Detailed bifurcation analysis with a simplified model for advanced heavy water reactor system. *Commun. Nonlinear Sci. Numer. Simul.* **2015**, *20*, 186–198.
11. Pandey, V.; Singh, S. A bifurcation analysis of boiling water reactor on large domain of parametric spaces. *Commun. Nonlinear Sci. Numer. Simul.* **2016**, *38*, 30–44. https://doi.org/10.1016/j.cnsns.2016.01.018.
12. Dhooge, A.; Govearts, W.; Kuznetsov, A.Y. MATCONT: A Matlab package for numerical bifurcation analysis of ODEs. *ACM Trans. Math. Softw.* **2003**, *29*, 141–164.
13. Dhooge, A.; Govaerts, W.; Mestrom, W.; et al. Cl_Matcont: A Continuation Toolbox in Matlab. In Proceedings of the 2003 ACM Symposium on Applied Computing, Melbourne, FL, USA, 9–12 March 2003; pp. 161–166.
14. Kuznetsov, Y.A. *Elements of Applied Bifurcation Theory*; Springer: Berlin/Heidelberg, Germany, 1998.
15. Kuznetsov, Y.A. *Five Lectures on Numerical Bifurcation Analysis*; Utrecht University: Utrecht, The Netherlands, 2009.
16. Govaerts, W.J. *Numerical Methods for Bifurcations of Dynamical Equilibria*; SIAM: Philadelphia, PA, USA, 2000.
17. Dubey, S.R.; Singh, S.K.; Chaudhuri, B.B. Activation functions in deep learning: A comprehensive survey and benchmark. *Neurocomputing* **2022**, *503*, 92–108. https://doi.org/10.1016/j.neucom.2022.06.111.
18. Kamalov, F.; Nazir, A.; Safaraliev, M.; et al. Comparative Analysis of Activation Functions in Neural Networks. In Proceedings of the 2021 28th IEEE International Conference on Electronics, Circuits, and Systems (ICECS), Dubai, United Arab Emirates, 28 November–1 December 2021; pp. 1–6. https://doi.org/10.1109/ICECS53924.2021.9665646.
19. Szandała, T. Review and comparison of commonly used activation functions for deep neural networks. In *Bio-Inspired Neurocomputing*; Springer: Singapore, 2020.
20. Sridhar. L.N. Bifurcation Analysis and Optimal Control of the Tumor Macrophage Interactions*. Biomed. J. Sci. Tech. Res.* **2023**, *53*, 45218–45225. https://doi.org/10.26717/BJSTR.2023.53.008470.
21. Sridhar, L.N. Elimination of oscillation causing Hopf bifurcations in engineering problems. *J. Appl. Math.* **2024**, *2*, 1826.
22. Flores-Tlacuahuac, A.; Morales, P.; Rivera-Toledo, M. Multiobjective Nonlinear model predictive control of a class of chemical reactors. *Ind. Eng. Chem. Res.* **2012**, *51*, 5891–5899.
23. Hart, W.E.; Laird, C.D.; Watson, J.P.; et al. *Pyomo—Optimization Modeling in Python*, 2nd ed.; Springer: Berlin, Germany, 2017; Volume 67.

24. Wächter, A.; Biegler, L. On the implementation of an interior-point filter line-search algorithm for large-scale nonlinear programming. *Math. Program.* **2006**, *106*, 25–57. https://doi.org/10.1007/s10107-004-0559-y.
25. Tawarmalani, M.; Sahinidis, N.V. A polyhedral branch-and-cut approach to global optimization. *Math. Program.* **2005**, *103*, 225–249.